



A digital moiré fringe method for displacement sensors^{*}

Jian WU, Ting-ting ZHOU, Bo YUAN^{†‡}, Li-qiang WANG

(State Key Laboratory of Modern Optical Instrumentation, CNERC for Optical Instrument, Zhejiang University, Hangzhou, 310027, China)

[†]E-mail: yuanbo@zju.edu.cn

Received Aug. 19, 2015; Revision accepted Feb. 16, 2016; Crosschecked Aug. 24, 2016

Abstract: In this study, a displacement measurement method based on digital moiré fringe is described and experimentally demonstrated. The method is formed by only one grating with a constant pitch. First, the magnified grating image is received by an imaging array and is sent to a computer. Then, the digital moiré fringes are generated by overlaying the grating image with its mirrored one. Finally, a specifically designed algorithm is used to obtain the fringes' phase difference before and after movement and calculate the displacement. This method has the effects of amplifying displacement and averaging the grating lines error, the same as the traditional moiré technique using two pieces of gratings. At the same time, the proposed system is much easier to assemble and the measurement resolution can be set more flexibly. One displacement measuring system based on this method was built up. Experiment results show that its measurement errors are less than 0.3 μm and less than 0.12 μm at the resolutions of 0.1 μm and 0.03 μm , respectively.

Key words: Digital moiré fringe, Displacement measurement, Grating

<http://dx.doi.org/10.1631/FITEE.1500270>

CLC number: TH741; TN911.7

1 Introduction

Displacement measuring technologies with the accuracy of submicron or nanometer level have received great attention since there is an extensive demand in various fields, such as metrology, industry, and scientific research (Zhao *et al.*, 2011; Khorshad *et al.*, 2012; Fleming, 2013). Among the measuring technologies, the grating-based displacement sensor has been more widely used in industrial manufacturing due to its long range, high resolution, immunity to electromagnetic interference, insensitivity to environmental conditions (e.g., dust, temperature, air flow), and low cost (Oka *et al.*, 2007; Lee and Jiang, 2013). Usually, moiré fringes are formed by overlaying two pieces of gratings with imaging or diffraction mode and then subdivided by subdivision circuits or software to attain a higher resolution in the

grating measuring system. Since two gratings are superimposed, their spatial orientations or gaps need to be precisely adjusted to detect the moiré fringes with high quality, for high accuracy measurement. The moiré fringe pattern generated by two gratings with slightly different periods was commonly used for alignment of mask and substrate in imprint lithography (Li *et al.*, 2006; Shao *et al.*, 2008). To achieve convenient adjustment and high overlay accuracy, the digital moiré fringes were focused in imprint lithography. Liu *et al.* (2006) overlaid a real grating with a virtual reference grating generated by a digital image to avoid the mismatch problem. Digital moiré fringes combined by two separate grating images were proposed for higher positioning accuracy in imprint lithography (Suehira *et al.*, 2007; Shao *et al.*, 2012). Digital moiré patterns with the digital grating images superimposed were also used in fields such as three-dimensional deformation measurement and displacement measurement (Wu *et al.*, 2014; Chen and Chang, 2015). The single-grating measuring methods were proposed to improve the grating-based displacement sensor and digital moiré fringes. In Yuan

[‡] Corresponding author

^{*} Project supported by the National Natural Science Foundation of China (No. 61205159)

ORCID: Jian WU, <http://orcid.org/0000-0001-9943-8341>

© Zhejiang University and Springer-Verlag Berlin Heidelberg 2016

et al. (2009) and Wang *et al.* (2015), an imaging array was employed to obtain only one grating image and its pixels were used for subdivision. However, this method totally abandons the ‘moiré pattern’ and the error averaging effect is relatively poor. The interferometer with a single grating was also proposed (Chu *et al.*, 2008; Cheng and Fan, 2011), in which two high-order diffraction beams were used to form interference fringe and CCD or photodetectors were employed to detect the fringe signals. Since this type of interferometer needs a coherent light source to obtain diffraction signals, it is sensitive to environmental conditions and is inclined to be affected by the local defect on the grating.

In the present study, a novel grating-based displacement measurement method is proposed, which uses digital moiré fringes formed by only one grating with a constant pitch. It has the advantages of convenient assembly, easy acquisition of high quality fringe signals, flexibility in setting the resolution, error averaging, and low cost.

2 Systemic configuration

The optical system using a single grating to measure displacement is shown in Fig. 1a. The grating is fixed on a motion platform and the grating line is perpendicular to the motion direction. The grating is illuminated by a collimated white-light source. Then, the image of the grating magnified by a lens is received by an imaging array, such as a CMOS or CCD image sensor. The magnifying power of optics should match the sizes of the grating pitch and the image sensor to guarantee that sufficient grating lines are captured by the image sensor. Usually, there is a small angle between the grating line and the row direction of the imaging array. The grating image signals are sent to the computer. Finally, a PC program generates digital moiré fringes and calculates the displacement.

The process of obtaining the digital moiré fringes is as shown in Fig. 1b. First, the mirrored grating image is generated by flipping the grating image along the row or column direction of the imaging array. Then, the digital moiré fringes are formed by overlaying the grating image and its mirrored image. Finally, two-dimensional digital moiré

fringes are integrated along the column direction to form one-dimensional digital moiré curves. The moiré curve is similar to a sinusoidal curve after it is averaged with a certain window size. The moiré curve is used to calculate the displacement.

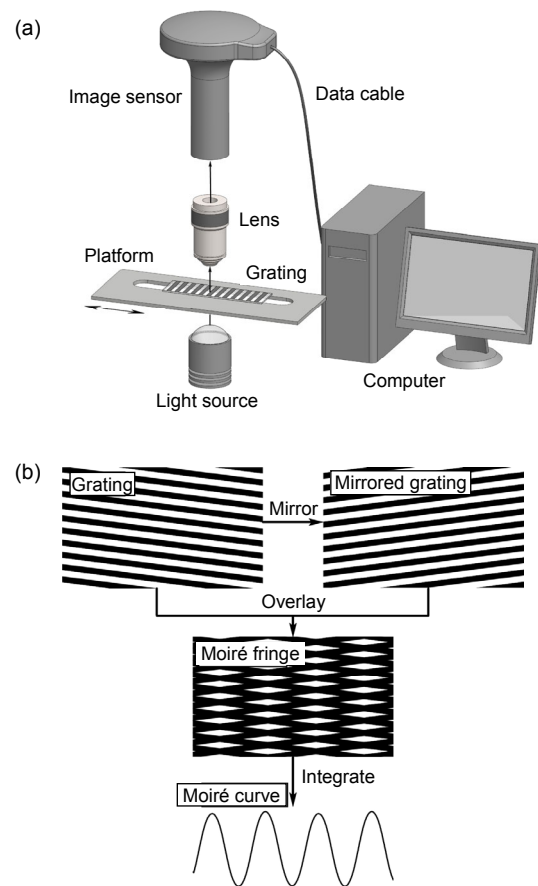


Fig. 1 Systemic configuration: (a) optical system; (b) formation of digital moiré fringes

3 Theoretical analysis

3.1 Displacement amplification

According to Fig. 1b, the digital moiré fringe has the function of displacement amplification. The principle here is slightly different from that of the traditional moiré fringe formed by two gratings (Fig. 2). The axes of x and y represent the row and column directions of the image sensor, respectively. The solid and dashed lines denote the grating image and its mirrored image, respectively. Suppose that the angle between the grating line and the x -axis is θ and

the grating pitch is p . The pitch of moiré fringe l can be obtained as

$$l = \frac{p}{2 \sin \theta} \tag{1}$$

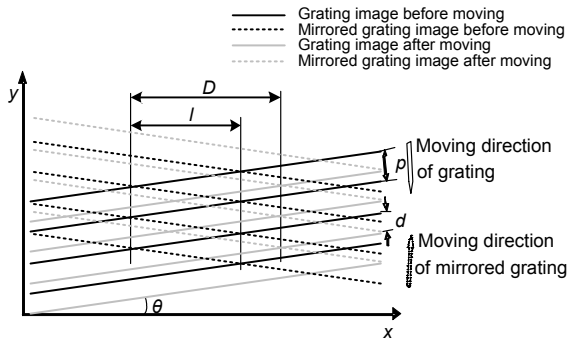


Fig. 2 Principle of displacement amplification

In Fig. 2, the black and gray lines denote the grating or mirrored grating before and after moving, respectively. Obviously, the mirrored grating moves in the opposite direction when the grating moves. It means that the digital moiré fringe moves two pitches as the grating moves one pitch. Thus, if the grating moves d , the moiré fringe moves

$$D = \frac{d}{\sin \theta} \tag{2}$$

So, the sensitivity of the digital moiré fringe is correlated with the rotation angle θ between the grating and the image sensor. The sensitivity is higher when θ is smaller, which will be discussed in Section 3.3.

3.2 Displacement calculation

The moiré curve in Fig. 1b can be expressed as

$$I = A \sin(\omega x + \varphi) + k, \tag{3}$$

where A , ω , φ , and k represent the amplitude, frequency, phase, and DC component of the curve, respectively. Suppose that φ_d is the difference of phases before and after movement. The moiré fringe moves $\varphi_d/(2\pi)$ pitches. So, the displacement of the moiré fringe is

$$D = l \cdot \frac{\varphi_d}{2\pi} \tag{4}$$

Combining Eqs. (1), (2), and (4), the grating displacement can be written as

$$d = \frac{p}{2} \cdot \frac{\varphi_d}{2\pi} \tag{5}$$

Phase difference φ_d can usually be expressed as

$$\varphi_d = 2n\pi + \Delta\varphi, \tag{6}$$

where n is the full-period counter and $\Delta\varphi$ is the phase difference within $(-2\pi, 2\pi)$. Eq. (5) shows that the key of displacement calculation is to obtain φ_d .

The phase φ in Eq. (3) can be estimated using conventional methods, such as those proposed in Ramos and Serra (2008) and Vucijak and Saranovac (2010). Here, a simple and efficient method for phase estimation is used (Fig. 3a). The moiré curve is normalized as $A=1$ and $k=0$ in the process of phase estimation. First, the frequency ω of measured moiré curve I is estimated using the peak-valley method, namely, calculating the average distance of adjacent peaks or valleys. Second, each discrete sinusoidal signal $I(i)$ with a phase of $i\omega$ is generated. Since the moiré curve is sampled by the image sensor, i must be an integer in the range of $[0, 2\pi/\omega)$. Then, the correlation coefficients of I and $I(i)$ are calculated and the estimated phase is that of $I(i)$ corresponding to the maximum correlation coefficient.

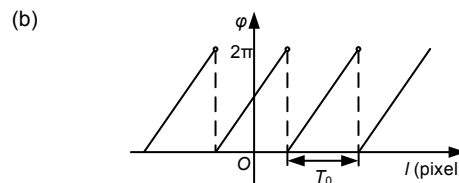
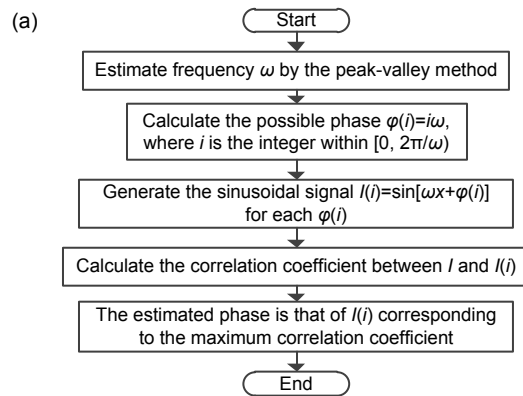


Fig. 3 Phase estimation (a) and the phase variation with the displacement of the moiré fringe (b)

Suppose that the phase of the digital moiré curve before moving is φ_b and that after moving is φ_a . $\varphi_a - \varphi_b$ is the phase difference $\Delta\varphi$ in Eq. (6). It is then necessary to record the full-period counter n . As shown in Fig. 3b, the phase variation with the displacement of the moiré fringe is a periodic sawtooth function when the grating is continuously moving in one direction. So, the full-period counter n should increase or decrease by one if the phase jumps down from 2π to 0 or jumps up from 0 to 2π , respectively.

3.3 Displacement resolution

Since the digital moiré fringe moves two periods as the grating moves one period, the displacement resolution can be expressed as

$$\delta = \frac{p}{2N}, \quad (7)$$

where N is the number of pixels occupied by one period of moiré curve.

However, the imaging system is not considered in Eq. (7). Suppose that the system magnifying power of the imaging system is β and that the pixel size of the imaging array is $b \times b$, the following equation can be obtained according to the object-image scale relation:

$$N \cdot b = \frac{\beta \cdot p}{2 \sin \theta}. \quad (8)$$

Combining Eqs. (7) and (8), the resolution δ can be expressed as

$$\delta = \frac{b \sin \theta}{\beta}. \quad (9)$$

Theoretically, the system resolution is higher when the pixel size b is smaller, the angle θ between the grating line and the row direction of the imaging array is smaller, or the magnifying power β is larger. However, the resolution cannot be improved unlimitedly. First, b is limited by the manufacturing technology for the imaging array. Second, if θ is too small, less than one period of the digital moiré curve is obtained, which makes it impossible to estimate the phase in Eq. (3). Third, if β is too large, a small number of grating lines are detected by the imaging

array, which weakens the error averaging effect of the moiré fringe and reduces the accuracy.

Once the detector and optical lens are fixed in one grating measuring system, b and β cannot be changed. However, it can still realize various resolutions by changing θ in Eq. (9). In practice, we need only to rotate the imaging array around the optical axis of the system.

4 Experiments and discussion

4.1 Experimental apparatus

Fig. 4 shows the hardware of the displacement measuring system based on the proposed principle. The grating is a general coarse metrology grating with a pitch of $20 \mu\text{m}$ and a length of 65mm . It was fixed on an Abbe comparator platform and the grating line was perpendicular to the motion direction of the platform. The Abbe comparator with a minimum division value of $1 \mu\text{m}$ was used only as a motion platform. So, it brings the same effects to the displacement sensors installed on the comparator, including the sensors for comparison and our displacement measuring system. The imaging array is a CMOS image sensor with 2048×1536 pixels and its pixel size is $3.18 \mu\text{m} \times 3.18 \mu\text{m}$. The output signals of the CMOS image sensor are transmitted via a USB interface. The imaging system consists of a $10\times$ objective and an eyepiece, and the system magnifying power is $6.48\times$. In the experiment, the displacement resolution was modified only by rotating the CMOS image sensor to change the angle θ . θ can be directly calculated from the grating image by a line detection algorithm commonly used in digital image processing. However, there will be only a few peaks and valleys in the digital moiré curve if θ is too small, which will lead to a large deviation of the frequency estimated according to the method described in Fig. 3a. We propose that the number of peaks and valleys in the curve should be larger than eight. The resolutions of $0.03 \mu\text{m}$ and $0.10 \mu\text{m}$ were used in the following experiments, and θ was set at 3.7° and 11.7° , respectively.

In experiments, two kinds of displacement sensors were used for comparison, since there are no available sensors that have high performance in terms of both displacement range and resolution.

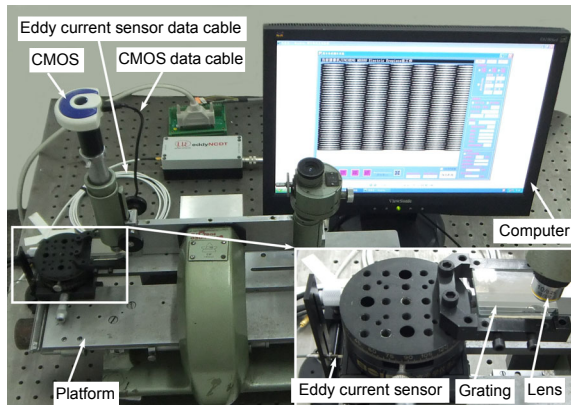


Fig. 4 The displacement measuring system

The eddy current sensor, eddyNCDT3010 (Micro-epsilon, Germany), was selected as one reference sensor for the tests on stability, sensitivity, and accuracy at a short displacement range. The measurement range is 0.5 mm and the resolution is 25 nm. Its output signals were collected by a 16-bit data acquisition card. To eliminate the effects of systemic noise and the environment, the signals were averaged for 2048 acquisitions.

The grating ruler, JCXE0.1 (Sinpo, China), was selected as another reference sensor for the test on systemic accuracy at a long displacement range (not shown in Fig. 4). Its measurement range is 200 mm and the resolution is 0.1 μm . The displacements were read directly from the digital display meter.

4.2 Quality of the digital moiré fringe

The high quality of the digital moiré fringe contributes to the displacement measurement accuracy, and the light source is an important factor affecting the quality. To investigate how much influence it has, the digital moiré fringes and the corresponding digital moiré curves were examined at various illuminations.

The systemic resolution was set at 0.03 μm . The Abbe platform was fixed and the digital moiré fringes were collected. Figs. 5a and 5b show the digital moiré fringes obtained at the illuminations of 100 lx and 390 lx, respectively. Although the digital moiré fringes are quite different, their normalized moiré curves are almost consistent (Fig. 5c), bringing almost no influence on phase estimation. Thus, it is easy to guarantee that the moiré fringe quality can meet the need for displacement measurement.

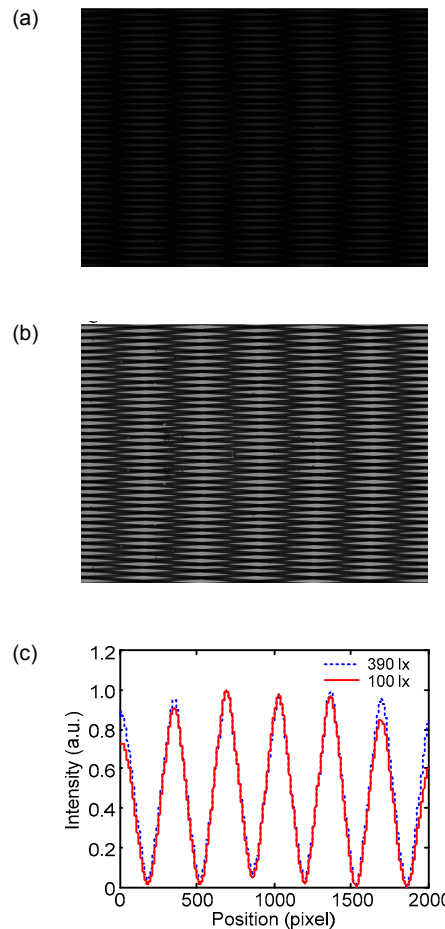


Fig. 5 Digital moiré fringes obtained at 100 lx (a) and 390 lx (b), respectively, and the corresponding digital moiré curves (c)

4.3 Stability

The stability of the measuring system will be affected by the light source, imaging array, environment condition, etc., which may increase the measurement error. Before investigating its stability, the Abbe platform was fixed for several hours to release the stress and become stable. The displacement resolution was set at 0.03 μm and the environmental temperature was stabilized at 29 $^{\circ}\text{C}$. The displacement values from the eddy current sensor and our measuring system were recorded every second for about half an hour. It can be seen from Fig. 6 that the displacement variation of our system is almost consistent with that of the eddy current sensor. Moreover, the displacement variation of our system does not exceed the resolution of 0.03 μm .

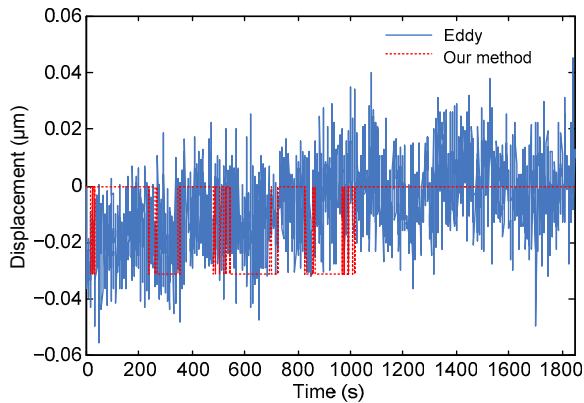


Fig. 6 Results of the stability test

4.4 Sensitivity

The sensitivity of the measuring system was tested by monitoring the movement of the platform in the unlocked status. If the platform is randomly moved to one position and is not locked, it slides at first and holds still finally because of the gap and the stress among the platform gears.

The measuring system was adjusted with the resolution being $0.03 \mu\text{m}$ and the environmental temperature stabilized at $29 \text{ }^\circ\text{C}$. The displacement values from the eddy current sensor and our measuring system were recorded every second for about 45 min (Fig. 7). It can be seen that the platform was moving slowly and returned to a stable status at last. Fig. 7 shows that our system is very sensitive to a small displacement and the sensitivity coincides with its resolution.

4.5 Displacement measurement accuracy

First, the measuring system was adjusted with the displacement resolution being $0.1 \mu\text{m}$ and was tested with the grating ruler. The displacements were recorded every $10 \mu\text{m}$ in the distance range of 3 mm. Fig. 8a shows the displacement errors between the grating ruler and our measuring system. It can be seen that the error is less than $0.3 \mu\text{m}$. Moreover, the standard error calculated from the displacement error curve is about $0.14 \mu\text{m}$.

Then, the measuring system was adjusted with the displacement resolution being $0.03 \mu\text{m}$ and was tested with the eddy current sensor. The displacements were recorded every $1 \mu\text{m}$ in the distance range

of $400 \mu\text{m}$. Fig. 8b shows the displacement error curves measured three times. It can be seen that the displacement error of the measuring system is less than $0.12 \mu\text{m}$ and that the calculated standard error is better than $0.05 \mu\text{m}$. Details about the results in Fig. 8b are shown in Table 1.

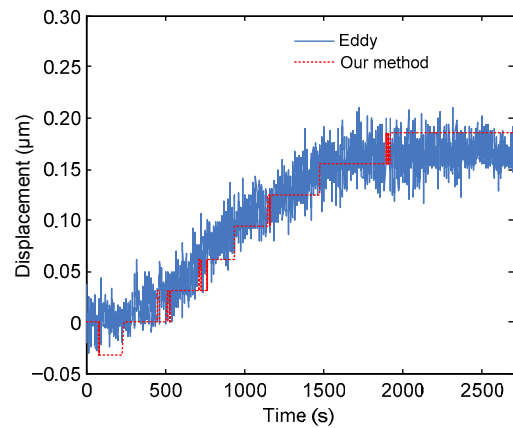


Fig. 7 Results of the sensitivity test

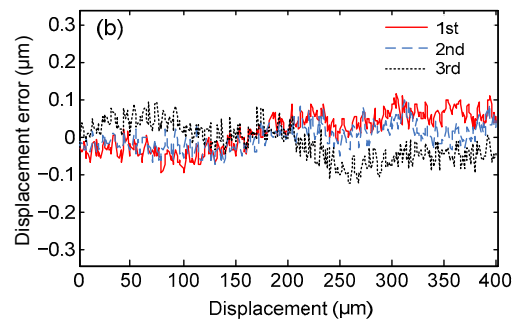
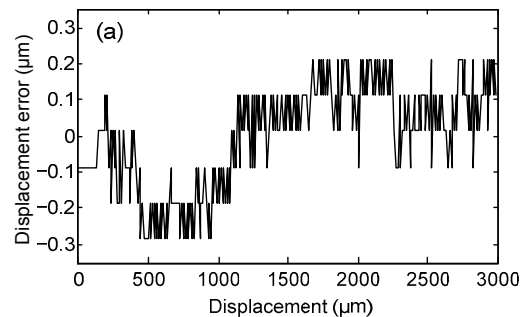


Fig. 8 Displacement error between the grating ruler and the measuring system with $0.1 \mu\text{m}$ resolution (a) and between the eddy current sensor and the measuring system with $0.03 \mu\text{m}$ resolution for each of the three measurements (b)

Table 1 Static results of measurements at the resolution of 0.03 μm

Test number	Maximum error (μm)	Standard error (μm)
1	0.12	0.05
2	0.10	0.03
3	0.12	0.05

5 Conclusions

A digital moiré fringe method was proposed for displacement measurement using only one metrology grating. The digital moiré fringe is formed by overlaying the grating image and its mirrored image, and a specifically designed algorithm is used to calculate the displacement. One displacement measuring system using the proposed method was tested at the resolutions of 0.1 μm and 0.03 μm , and the errors are no more than 0.3 μm and no more than 0.12 μm , respectively. The advantages of the displacement sensor based on the digital moiré fringe method are:

1. The method can magnify the displacement and weaken the measurement error caused by the local grating defects and some random factors, which are the same as the traditional moiré fringe technology. This is because the formation of digital moiré fringes is similar to that of traditional moiré fringes except that one virtual grating (i.e., the mirrored grating) is introduced in the present method.

2. Since only one grating is used in the proposed system, the system is easier to assemble and the measurement error caused by the interval between two gratings can be totally eliminated. Additionally, the moiré signal obtained from one grating has a higher quality than that from two gratings.

3. The systemic resolution can be changed by rotating only the imaging array for different applications, without any hardware replacement. By contrast, the existing grating ruler generally has a fixed resolution and one needs various rulers to meet different measurement accuracies.

4. Compared with the systems having the same resolutions, our proposed system is simpler and costs less. The digital moiré fringes are directly subdivided by the pixels of the imaging array. There is no need to design an extra processing circuit for subdivision.

References

- Chen, X.X., Chang, C.C., 2015. A digital sampling moiré method for two-dimensional displacement measurement. *SPIE*, **9435**:943523.
<http://dx.doi.org/10.1117/12.2084148>
- Cheng, F., Fan, K.C., 2011. Linear diffraction grating interferometer with high alignment tolerance and high accuracy. *Appl. Opt.*, **50**(22):4550-4556.
<http://dx.doi.org/10.1364/AO.50.004550>
- Chu, X.C., Lü, H.B., Zhao, S.H., 2008. Research on long-range grating interferometry with nanometer resolution. *Meas. Sci. Technol.*, **19**(1):017001.
<http://dx.doi.org/10.1088/0957-0233/19/1/017001>
- Fleming, A.J., 2013. A review of nanometer resolution position sensors: operation and performance. *Sens. Actuat. A*, **190**:106-126.
<http://dx.doi.org/10.1016/j.sna.2012.10.016>
- Khorshad, A.A., Hassani, K., Tavassoly, M.T., 2012. Nanometer displacement measurement using Fresnel diffraction. *Appl. Opt.*, **51**(21):5066-5072.
<http://dx.doi.org/10.1364/AO.51.005066>
- Lee, J.Y., Jiang, G.A., 2013. Displacement measurement using a wavelength-phase-shifting grating interferometer. *Opt. Expr.*, **21**(21):25553-25564.
<http://dx.doi.org/10.1364/OE.21.025553>
- Li, N.H., Wu, W., Chou, S.Y., 2006. Sub-20-nm alignment in nanoimprint lithography using moiré fringe. *Nano Lett.*, **6**(11):2626-2629. <http://dx.doi.org/10.1021/nl0603395>
- Liu, C.M., Chen, L.W., Wang, C.C., 2006. Nanoscale displacement measurement by a digital nano-moiré method with wavelet transformation. *Nanotechnology*, **17**(17):4359-4366.
<http://dx.doi.org/10.1088/0957-4484/17/17/012>
- Oka, T., Ohmura, Y., Nakajima, H., et al., 2007. Displacement sensor based on grating imaging with a cylindrical lens array and a phase grating. *Opt. Eng.*, **46**(7):073603.
<http://dx.doi.org/10.1117/1.2753185>
- Ramos, P.M., Serra, A.C., 2008. A new sine-fitting algorithm for accurate amplitude and phase measurements in two channel acquisition systems. *Measurement*, **41**(2):135-143.
<http://dx.doi.org/10.1016/j.measurement.2006.03.011>
- Shao, J., Liu, H., Ding, Y., et al., 2008. Alignment measurement method for imprint lithography using moiré fringe pattern. *Opt. Eng.*, **47**(11):113604.
<http://dx.doi.org/10.1117/1.3028350>
- Shao, J., Ding, Y., Tian, H., et al., 2012. Digital moiré fringe measurement method for alignment in imprint lithography. *Opt. Laser Technol.*, **44**(2):446-451.
<http://dx.doi.org/10.1016/j.optlastec.2011.08.010>
- Suehira, N., Terasaki, A., Okushima, S., et al., 2007. Position measurement method for alignment in UV imprint using a high index mold and "electronic" moiré technique. *J. Vac. Sci. Technol. B*, **25**(3):853-856.
<http://dx.doi.org/10.1116/1.2737440>
- Vucijak, N.M., Saranovac, L.V., 2010. A simple algorithm for

- the estimation of phase difference between two sinusoidal voltages. *IEEE Trans. Instr. Meas.*, **59**(12):3152-3158.
<http://dx.doi.org/10.1109/TIM.2010.2047155>
- Wang, H., Wang, J., Chen, B., et al., 2015. Absolute optical imaging position encoder. *Measurement*, **67**:42-50.
<http://dx.doi.org/10.1016/j.measurement.2015.02.028>
- Wu, D., Xie, H., Li, C., et al., 2014. Application of the digital phase-shifting method in 3D deformation measurement at micro-scale by SEM. *Meas. Sci. Technol.*, **25**:125002.
<http://dx.doi.org/10.1088/0957-0233/25/12/125002>
- Yuan, B., Yan, H.M., Cao, X.Q., 2009. A new subdivision method for grating-based displacement sensor using imaging array. *Opt. Lasers Eng.*, **47**(1):90-95.
<http://dx.doi.org/10.1016/j.optlaseng.2008.07.013>
- Zhao, S., Hou, C., Bai, J., et al., 2011. Nanometer-scale displacement sensor based on phase-sensitive diffraction grating. *Appl. Opt.*, **50**(10):1413-1416.
<http://dx.doi.org/10.1364/AO.50.001413>